Undergraduate Senior Project

Fabrication and Characterization of Single -Walled Carbon Nanotube Thin Films for Optical Sensing Applications

Kanokwan Klahan

Suporvisor: Dr. Yodchay Jompol

Department of Physics, Faculty of Science, Mahidol University

June 16, 2020

Fabrication and Characterization of Single - Walled Carbon Nanotube Thin Films for Optical Sensing Applications

Kanokwan Klahan

Abstract

Optical sensors that available in the sensor market have various functions, e.g., position sensors, automatic-night lamps, gas sensors, and biomedical sensors. Mostly, the direct bandgap semiconductors are used to make optical devices. Depending on their structures, single-walled carbon nanotubes (SWCNTs) can behave as direct bandgap semiconductors or metals. They possess very fascinating properties such as high carrier mobility, high thermal conductivity, and good mechanical strength. They also exhibit strong interaction with photons. There are many studies on single-walled carbon nanotube films for numerous applications, e.g., sensors, energy conversion, and transparent conductive electrodes.

In this project, we fabricated and characterized single-walled carbon nanotube based thin films for optical sensing applications in particularly photoconductor or photo-resistor. SWCNTs thin films were fabricated via spin coating which is simple solution deposition techniques. The devices were then characterized under a normal condition (room temperature and atmospheric pressure) and light illumination in the aspects of the optical and electrical property. We observed the change in the electrical behavior of SWCNT thin film under light illumination. This indicates that our SWCNT based thin films may have the potential to be used as optical sensors with further studies and modifications. We also made use of SWCNT thin films as conductive electrodes to fabricate a more complex device, i.e., supercapacitors. We found that the fabricated supercapacitors have capacitances in the order of microfarad. Cyclic voltammetry curves confirmed the charge-discharge process in our supercapacitors.

Keywords: Single-walled carbon nanotube, optical sensor, thin film, supercapacitor

Acknowledgment

First of all, I would like to thank my supervisor, Dr. Yodchay Jompol, for the patient guidance, assistance, encouragement, and advice he has provided throughout my time as his student. Then I would like to thank all the graduate students, Mr. Momgkol Saphankeaw and Mr. Chan Thar Soe, in our laboratory for the advice during my research, the instruction, and suggestions on how to use any equipment and machines in a kindly way. I very much appreciate their help and support. I also want to thank Sritrungthong scholarship from the Faculty of Science, Mahidol University for the financial supports throughout the period as an undergraduate student. Finally, I would like to thank all my friends and family for their support.

Contents

List of Figures

List of Tables

Introduction

1.1 Motivation

Nowadays, there are many types of optical sensors available in the sensor market. These devices have various advantages and functions, e.g., position sensors, automatic-night lamps, gas sensors, and biomedical sensors. The most common types of optical sensors or photodetectors include photo-resistors light-dependent resistors, photovoltaic devices, photodiodes, and phototransistors [1]. Their working principle is based on the interaction between charge carriers in semiconducting materials and photons. Mostly, the direct bandgap semiconductors (e.g., InAs, GaAs, CdS) are used to make optical devices. It is because charge carriers or electron-hole pairs of direct bandgap materials can be simply produced by photons. Depending on their diameters and structures, single-walled carbon nanotubes (SWCNTs) can behave as direct bandgap semiconductors or metals. They possess very fascinating properties such as high carrier mobility, high thermal conductivity, and good mechanical strength. They also exhibit strong interaction with photons [2]. Optical detectors based on individual SWCNT have been investigated in many studies. Carbon nanotube films have also been studied for numerous applications, e.g., sensors, energy conversion, and transparent conductive electrodes [3]. In the film fabrication process, there are many techniques and methods. However, it is much more convenient and easier to rely on the solution-based deposition, e.g., spray coating, spin coating, dip coating. Since we want to fabricate uniform thin films of SWCNTs, spin coating technique is the most suitable method.

With these advantages from SWCNTs properties and fabrication process, we were convinced to investigate and study the properties and applications of single-walled carbon nanotube based thin films fabricated by spin coating for optical sensing applications particularly photoconductor or light-dependent resistor. Considering the use of the optical sensor and photodetector, they are mostly used in the real environment. Therefore, it is more desired to have some protective layer on the active area of SWCNT films. Therefore, the properties of SWCNT thin films with a protective layer should also be studied and investigated. Finally, due to the high surface areas and high electrical conductivity of SWCNTs, we can use SWCNT thin films to demonstrate them as the transparent conductive electrode in supercapacitors.

1.2 Objectives of the research

1. To fabricate carbon nanotube thin films with spin coating method for optical sensing applications
2. To investigate and characterize optical and electrical properties of carbon nanotube thin films
3. To observe the change in electrical properties of SWCNT thin films under light illumination
4. To demonstrate the use of SWCNT thin films as conductive electrode in supercapacitors

Background Knowledge

2.1 Single - Walled Carbon Nanotubes (SWCNTs)

Discovered and first characterized in 1991 by Iijima [4], carbon nanotubes are one of the carbon allotropes since they are composed only of carbon atoms. Generally, carbon nanotubes are divided into two types, single-walled carbon nanotubes (containing only one layer) and multi-walled carbon nanotubes (containing more than one layer). For SWCNTs, their shapes are cylindrical with the diameter ranging in nanometers and length from nanometer to micrometer (or even centimeter). MWCNTs are also cylindrical shape but their sizes are way larger.

Structure and Property of single - walled carbon nanotube

Single - walled carbon nanotubes are widely known as one - dimensional materials. They consist of a sheet of graphene, rolled up to form hollow tubes with walls only one atom thick [figure 2.1a]. Because of their structures and dimension, the properties of SWCNTs are exceptional from bulk materials, e.g., mechanical strength, electrical, thermal, and optical properties.

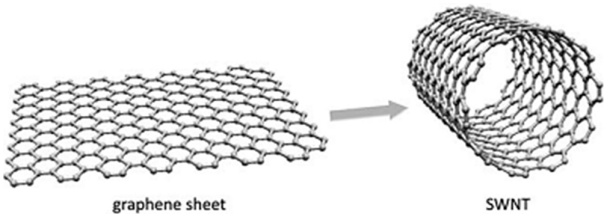

(a) Structure of single - walled carbon nanotube

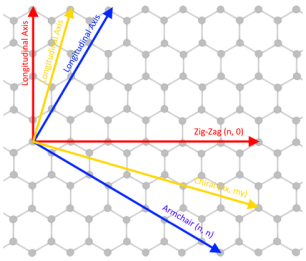

(b) Direction or lattice orientation that graphene is rolled to form SWCNTs (adapted from [5])

Figure 2.1: Structure of each type of single - walled carbon nanotube

The electrical behaviors, metallic or semiconducting, of SWCNTs are dependent upon the direction that graphene is rolled or the lattice orientation. As shown in figure 2.1b, SWCNTs can be classified into 3 types, zig-zag, armchair, and chiral (any direction other than zig - zag and armchair) depending on their structures and lattice orientations. The lattice orientation is noted by a pair of integers (n, m) which defined the chiral vector. SWCNTs show metallic behavior when the condition of $n - m = 3l$ is met where l is an integer, otherwise semiconducting behavior is shown [4]. Following this condition, it can be concluded that armchair carbon nanotubes are always metal. Besides, zig - zag and chiral carbon nanotubes can behave as a semiconductor or metal depending on the chiral vector.

In figure 2.2, the density of state of the metallic and semiconducting nanotube is shown. For metallic SWCNTs, there is density of state presented around the center. On the other hand, there is a bandgap that has zero density of state in semiconducting SWCNT. Band structure of semiconducting SWCNT demonstrates the direct bandgap property of SWCNT

as we can see that the top of the conduction and the bottom of the valence band are at the same momentum, k. This direct bandgap property of SWCNT has advantages in optical sensing applications, photonic, and optoelectronic. It is worth mentioning that the bandgap energy of SWCNT depends on tube diameter, structure, electrical transition.

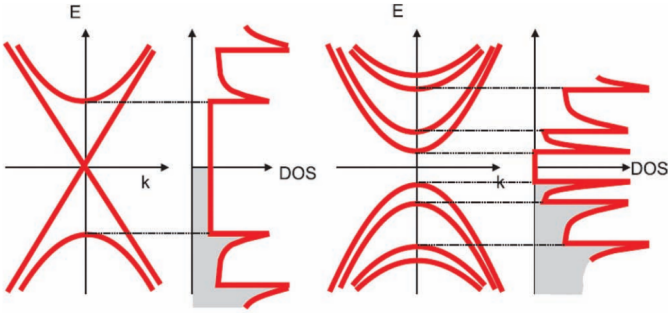

Figure 2.2: Density of state and band structure of metallic (left) and semiconducting (right) single - walled carbon nanotube (adapted from [2])

2.2 Supercapacitors

Capacitors are one of the electrical circuit elements used to store electrical energy. Considering the simplest form of conventional capacitors, it consists of two conductive electrodes and a dielectric layer. The energy is stored by the accumulation of charges at the electrode. In contrast to the conventional capacitor, the Electrical Double Layer Capacitor (EDLC) which is a type of supercapacitors contains no conventional dielectric. The layer between conductive electrodes is instead filled with an electrolyte which has many free electrons or ions. Considering the charge and discharge process in EDLC, there is the formation of "electrical double layer" at the interface between the electrodes and electrolyte during the charging process. These make supercapacitors to have high power density and storage capacity.

Particularly, the capacitance of EDLC capacitor is proportional to the surface area of the electrical double layer. So, to achieve high capacitance of EDLC cell, it is required large surface are materials as electrodes. The mechanism of ion absorption and desorption at the interface between electrodes and an electrolyte gives rise to charge and discharge of EDLC. By applying a voltage to the electrode, many ions move to the interface of the electrical double layer and the EDLC capacitor is then charged. When discharging or connecting EDLC cells to electrical elements, ions will move conversely from the direction in the charging process as shown in figure 2.3. Normally, EDLC consists of electrodes, electrolyte, and the separator which prevents facing electrodes from contacting each other and is optional.

To determine the capacitances of supercapacitors, there are various techniques and methods, i.e., galvanostatic method or charge - discharge, cyclic voltammetry (CV), and electrochemical impedance spectroscopy (EIS). However, the imperfections and defects in the materials used in the construction of the capacitor have very significant effects on the performance of capacitors. Impedance, dissipation factor, inductive reactance, equivalent series

resistance, and leakage current are used to characterize and determine the imperfections and defects in capacitors. For instance, equivalent series resistance (ESR) and leakage current are modeled as inter resistance series and parallel with capacitor cells, respectively. In this section, we would like to mention only about cyclic voltammetry technique and leakage current.

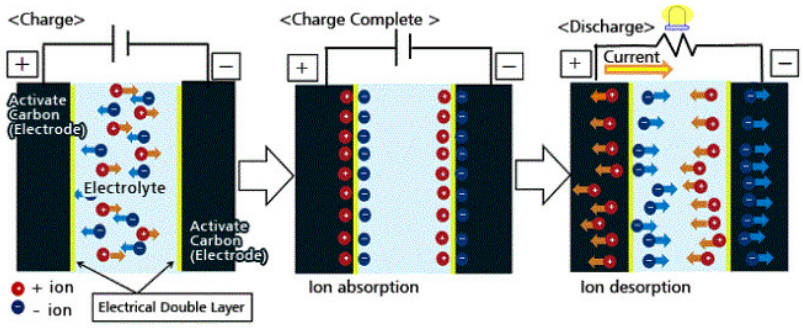

Figure 2.3: Diagram illustrating supercapacitor structure and working mechanisms (adapted from [6])

Cyclic voltammetry and evaluation of capacitance

Cyclic voltammetry (CV) is a powerful tool and popular electrochemical technique. Generally, it is utilized to investigate the reduction and oxidation processes. It is also one of the techniques widely used in determining capacitance because it can study and show the reaction that happens during the charge and discharge process. In figure 2.4, the example CV curve obtained from a capacitor is shown. The curvature indicates the redox reaction at the interface between electrode and electrolyte. This redox reaction is linked to the ions adsorption and desorption at the electrical double layer which is also linked to the charge and discharge process of a capacitor. Cyclic voltammetry is performed by circulating voltage from specific voltage to voltage with a certain value of voltage scan rate and then measuring the resulting current.

Following the equation 2.1 and 2.2 [7], [8], the capacitance can be calculated from CV curve because the integral term is determined from area under CV curve. The capacitance obtained from CV can be varied in the same sample with different parameter, e.g., scan rate, potential window. The slower scan rate will give rise to the greater capacitance.

$$C_s = \frac{1}{S\nu\Delta V}\int_{V_1}^{V_2} IdV \tag{2.1}$$

$$C = SC_s = \frac{1}{\nu\Delta V}\int_{V_1}^{V_2} IdV \tag{2.2}$$

Where C_s is specific capacitance in F/m^2, C is capacitance in F, S is electrode area, ν is voltage scan rate, and ΔV $(V_2 - V_1)$ is potential window.

Leakage current of supercapacitors

In ideal capacitors, the dielectric materials are perfect insulator which means that they don't allow any current to leak through capacitors or themselves. In contrast to real capacitors, there are some impurities and defects in dielectric materials that cause current to be

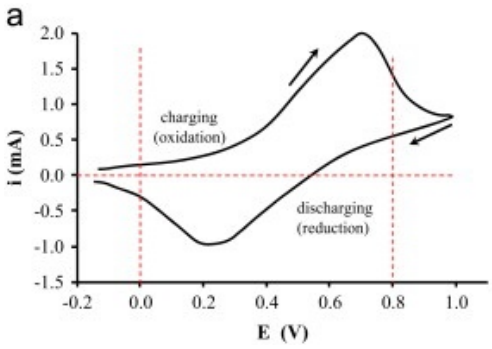

Figure 2.4: Example of CV curve of a capacitor (adapted from [9])

able to pass through. This current is referred to as DC leakage current that flows through a capacitor when voltage is applied. Its value can be varied depending on temperature, voltage, and charging period. So, it is better to obtain less leakage current which leads to less loss in power stored within a capacitor. The simplified mathematical model of a real capacitor is shown in figure 2.5

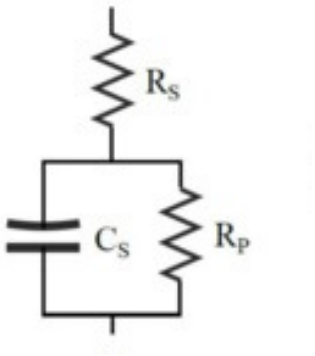

Figure 2.5: The simplified mathematical model of real capacitor (adapted from [10])

2.3 Spin Coating Technique

What is spin coating?

Spin coating is the method used to fabricate thin film on to substrates. It is a simple technique and able to assemble uniform thin films. Normally, the solution or colloid consisted of solvent and solute/particles which are the substance that we want to fabricate it as a film, are deposited onto the substrate. After dispensation of the solution, the substrate is radially accelerated and spun at a very high speed. The solution will be spread over and off the substrate surface by centrifugal force (a force that acts outward on an object moving around a center). Then, the solvent in solution left on the substrate evaporates leaving a thin film of solute/particles on the substrate. The thicknesses of films can be adjusted into the order of nanometer to micrometer by changing the protocol, e.g., spin speed, spin acceleration, spinning time, and set of spin step [11].

Processes of spin coating technique

Figure 2.6: Spin coating machine

The process and stage of operation can be divided into 4 parts including dispensation, spin acceleration, constant spin speed, and evaporation.

1. Dispensation

   In this step, the mixture is dispensed and covered all over a substrate. It can be classified into two types, i.e., dynamic dispensation and static dispensation [12]. Dynamic dispensation is done by dropping the mixture while the substrate is spinning at a very low speed. For static dispensation, the mixture is spread ed over a substrate by using the tip of pipette or dropper.

2. Spin acceleration

   To get more even coverage of mixture on substrates and thin films, the mixture or solution on substrates are radially pulled off from substrates by centrifugal force. This centrifugal force is generally generated from the spinning of a substrate.

3. Constant spin speed

   After accelerating the substrate for amount of time until the required spin speed is reached, the substrate will spin at a constant spin speed. The mixture is still spread off over the edge of a substrate before the equilibrium is reached. The equilibrium point happens when viscous shear drag force from the mixture (which is inward direction) balances centrifugal force [11]. These processes thin and define the thicknesses of films.

4. Evaporation

   This is the stage where solvent is removed and then there's only the substance left on a substrate while the substrate is still spinning. The evaporation stage doesn't define film thicknesses because only the solvent is removed.

It is worth to mentioning that there can be more than one step in operations or protocols. In one step, it's consisted of spin acceleration, spin speed, and spinning time. We can design the protocol by combining these steps to get the desired films.

Effects of parameters on films fabricated by spin coating

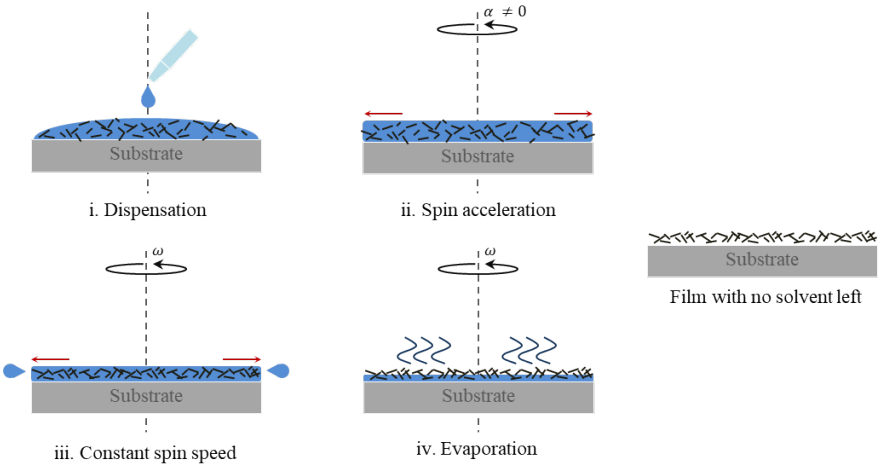

Figure 2.7: Diagram illustrating spin coating stage

1. Spin speed, viscosity of solution, and solution concentration

   Referring to the previous theoretical studies on spin coating technique [13]–[15], it can be concluded that the film thickness, t, depends on spin speed and solution properties like the following equation.

$$t \propto \frac{\eta^{1/3} c}{\sqrt{\omega}} \tag{2.3}$$

   Where t is film thickness, η is viscosity of solution, c is solution concentration, and ω is spin speed.

   As we can see from equation (2.3), the thickness of films can be varied by changing spin speed and solution properties, i.e., viscosity and concentration. By increasing spin speed for the same solution, the thicknesses will become thinner. If we use the same protocol for solutions that have different viscosities and concentrations, the more concentrate or viscous the solution is, the thicker the film becomes.

2. Substrates

   The choice of substrates used in the fabrication process is also a key factor in the film properties, e.g., uniformity, coverage, and defect. Normally, the substrates are chosen so that the solution can wet the substrates which in turn gives the good coverage during dispensation process. If the solution is water - based solution, the substrate should be hydrophilic materials.

2.4 Sputtering Technique

What are sputtering technique and DC sputtering?

Sputtering is one of the widely used manufacturing processes in many industries, e.g. semiconductors, electronics, and optical devices [16]. It is used to deposit thin films on substrates. In the sputtering process, the atoms are ejected from a target by the bombardment of high energy particles, particularly electron and ion in the electric or magnetic field. The target material could be solid or liquid. Sputtering process can be divided into many types

based on the energy source, manipulation of the atom diffusion, and so on [17]. DC sputtering is sputtering process that uses direct current and also high voltage to apply at a target to generate bombarding particles. Generally, this process is for the deposition of conductive targets/materials on a substrate.

Principle of DC sputtering

1. The process is done in the vacuum chamber containing specific gas species which is usually an inert gas.
2. High negative voltage, i.e. electron is applied to the target material and the substrate holder is grounded. So, there will have an electric field between a target and a substrate.
3. Free electrons flow from the negatively charged target to the substrate holder. These electrons then collide with outer shell electrons of the inert gas atoms.
4. The inert gas atoms become positively charged and move to (the same as electric field direction) and collide the target at very high velocities.
5. Due to the bombardment of high energy - momentum particles, the particles are sputtered off from the target. Finally, these particles diffuse through the chamber and deposit onto the substrate.
6. During these processes, the plasma is created from high energy particles moving around and ionisation of gas atoms.

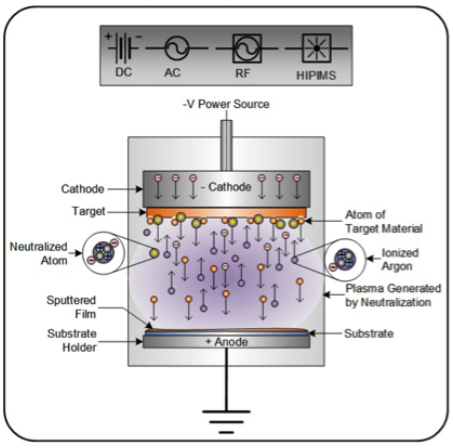

(a) Diagram of sputtering process [17]

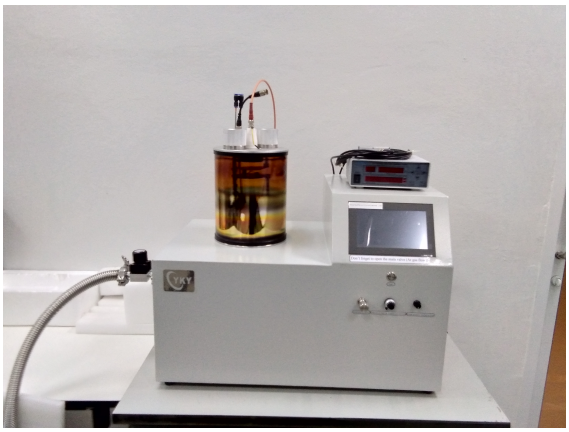

(b) DC sputtering machine

Figure 2.8: Diangram of sputtering process and DC sputtering machine

Operation process of DC sputtering

The operation process of DC sputtering is involved with the low - pressure process because the system inside the operating chamber is needed to be specific and controlled. The following processes is the brief operations used in this works. Note that these processes can be varied depending on the purposes of works.

1. Firstly, the chamber is evacuated until the pressure inside is in the order of 1 Pa. Then, the operating gas (which is the gas required to set the system during sputtering) flows into the chamber to the certain pressure for 15 minutes.

2. The operating gas then is turned off. After that, the procedure above is repeated. The aim of these procedures are to get rid of unwanted particles/gases in the chamber and sputtering process.

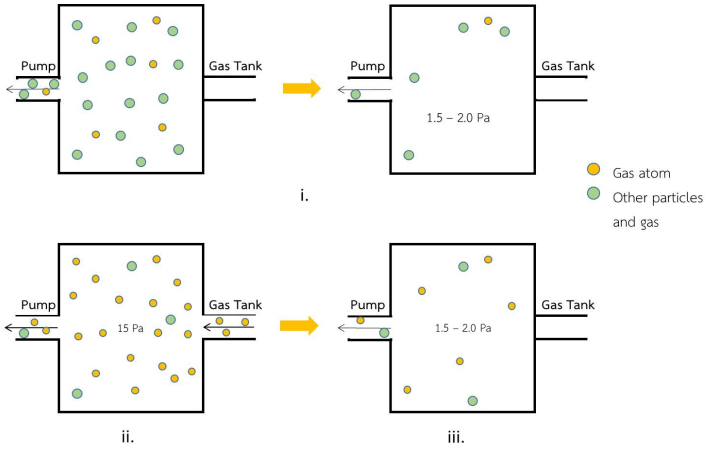

Figure 2.9: Diagram illustrating pre - operation before sputtering

3. There are amount of parameters that need to be set before sputtering which is varied based on target materials and so on.
   - Operating pressure: the pressure inside the chamber during sputtering
   - Sputtering time: the amount of time used in sputtering
   - Plasma current/ pressure
4. Pre-sputter for certain amount of time depending on the target material. In this step, the plasma shutter is placed between the target and substrate. So, there are no atoms from the target deposited on the substrate.
5. Plasma shutter's then removed so that target atoms can diffuse and deposit onto substrates.

Effects of parameters on films deposited by DC sputtering

Some factors and parameters determine the quality and defect of film deposited by DC sputtering. In this section, some of them are discussed.

1. Substrates

   The adhesion between substrates and target atoms should be good enough that the deposited films will not fall out from substrates. Moreover, they are needed to be suitable for sputtering process which copes with a certain amount of heat and plasma jet.

2. Pre - operation before sputtering

   During sputtering process, the system inside the operating chamber is needed to be ideal as much as possible. In this context, the ideal system is that there is only operating gas inside the chamber. If other gas species are present, it will cause the imperfection of material. For instance, if the target is easily oxidized metal and there is too much oxygen inside the chamber, the deposited film will contain both metal and metal oxide.

So, it is essential to do pre - operation strictly to get rid of other gases from the chamber as much as can be achieved.

3. Operating pressure

   Since target atoms need to diffuse onto a substrate to form a film, the diffusion of target atoms is important. Besides, the operating pressure can affect atom diffusion. So, we need to determine the appropriate operating pressure for a specific target material.

4. Plasma current/pressure

   This factor has effects on film properties almost the same as the operating pressure. Moreover, it also relates to the bombarding energy at a target material.

5. Sputtering time

   Sputtering time directly affects thicknesses of films. The more sputtering time, the thicker the film becomes.

6. Target material

   For different materials, the sputtering protocols are varied because of their different properties, e.g., diffusion rate, binding energy, and oxidization rate.

Experimental Considerations

In this part, we discussed fabrication processes and characterizations of devices. SWCNT based devices studied and fabricated in this work were SWCNT thin films and supercapacitors based on SWCNT electrodes. We have fabricated different configurations of SWCNT thin films and investigated their properties. We fabricated SWCNT thin films with different electrode configurations, i.e., symmetrical (both contacting electrodes are the same), and asymmetrical electrode (each contacting electrode is different). We also fabricated SWCNT thin films with and without polymer coating or protective layer. Poly(vinyl alcohol) or PVA for short was used to coat SWCNT thin films in this work. We then demonstrated the use of SWCNT thin films as electrodes for supercapacitors with different types of PVA based - gel electrolytes. The overview of devices fabricated and studied in this work is shown in fig 3.1.

In this work, spin coating technique was utilized to produce SWCNT thin films and coat other materials (PVA solution and PVA based – gel electrolyte) for preparations of both type devices. Contacting electrodes for the measurement and characterization of the devices was fabricated using sputtering method.

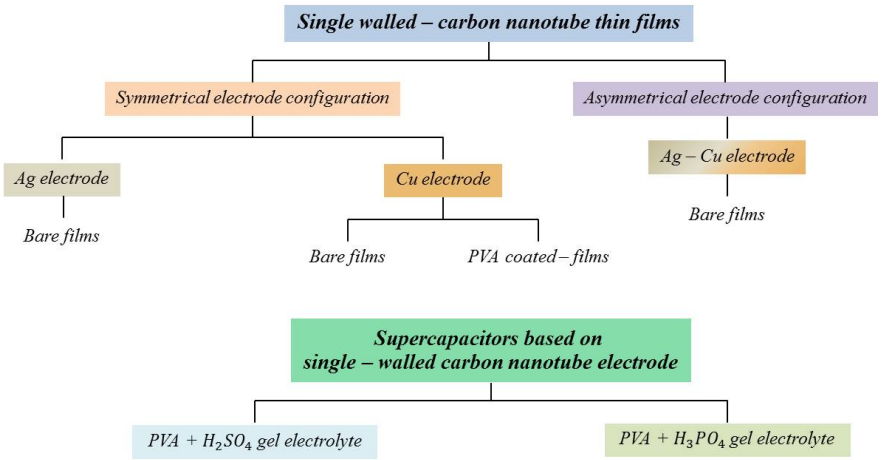

Figure 3.1: Overview of devices that were fabricated and studied

3.1 Single - Walled Carbon Nanotube Thin Films

3.1.1 Device configuration

In figure 3.2, the configurations of SWCNT thin film devices were shown. Firstly, SWCNT films were fabricated on glass substrates. Then, contacting electrodes were deposited on SWCNT films. For PVA coated SWCNT thin film devices, PVA solution was coated after the preparation of SWCNT film and contacting electrodes.

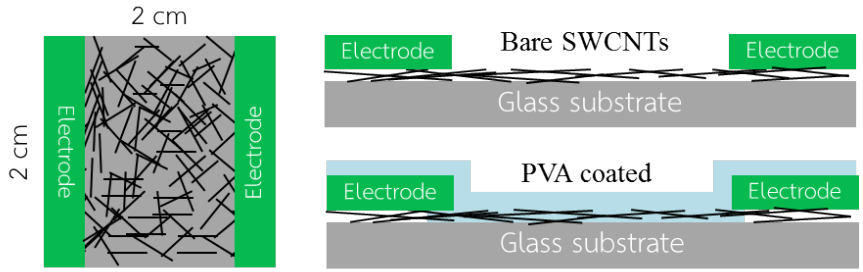

Figure 3.2: Configuration of single - walled carbon naotube thin films

3.1.2 Preparation of single - walled carbon nanotube thin films

Carbon nanotube solution

1. Properties of single - walled carbon nanotube solution

   Single - walled carbon nanotube solution was purchased from *Time Nano, Chengdu Organic Chemicals Co.Ltd.,Chinese Academy of Sciences* in 2013. The initial concentration of SWCNT content in the solution was 1 mg/ml. The making method of SWCNT was chemical vapor deposition with methane catalytic decomposition over a Co-based catalyst. In this solution, there were both **metallic and semiconducting** single - walled carbon nanotubes. The table 3.1 shows the properties of SWCNTs in the solution.

   I_d/I_g ratio is the intensity ratio between D peak and G peak in Raman spectrum of SWCNTs. This value indicates defect density in the material. The lower I_d/I_g ratio, the lower defect density.

Property	Unit	Value
Outer Diameter	nm	<2
SWCNTS purity	wt %	>95
Length	μm	5 - 30
Specific surface area	m^2/g	>490
Electrical conductivity	s/cm	>100
I_d/I_g	-	<0.05

Table 3.1: Properties of SWCNTs content in solution

Optical absorption of Single-wlled carbon nanotube solutions

The measurement was done by using UV-Vis spectroscopy. The optical absorption spectra in the photon energy domain, $E_{photon} = 1239.8/\lambda(\text{nm})$, of SWCNT solutions with different concentrations are shown in figure 3.4.

2. Variation of SWNCNT concentration

Figure 3.3: Single - walled carbon nanotube solution

From equation 2.3 [13]–[15], SWCNT concentrations were varied by diluting stock solution with distilled water to vary film thickness and denseness. The variation of SWCNT concentration and the notation of film made from a certain SWCNT concentration are shown in table 3.2. CNT:DI is the ratio between the volume of stock solution and distilled water in the dilution process.

	CNT : DI	Concentration (mg/ml)
S32	3:2	0.6
S11	1:1	0.5
S12	1:2	0.333
S15	1:5	0.167
S110	1:10	0.091

Table 3.2: Variation of SWCNT concentrations used in film preparations

Single - walled carbon nanotube thin film fabrications

In film fabrication process, spin coating technique was utilized to get SWCNT thin films with variations of thickness and denseness.

1. Substrates
   i. In this work, SiO_2 or glass substrates were used as substrate with 2 × 2 cm in size.
   ii. Cleaning process of substrates
      1) The substrates were put in acetone and sonicated in an ultrasonic bath under 5 minutes and 35 degree Celsius.
      2) Then, the substrates were rinsed with Isopropyl alcohol and distilled water, respectively.
      3) The procedure mentioned above was repeat 2 times.
      4) Finally, the substrates were blow with nitrogen gas.
2. Protocol for single - walled carbon naotube thin film fabrication

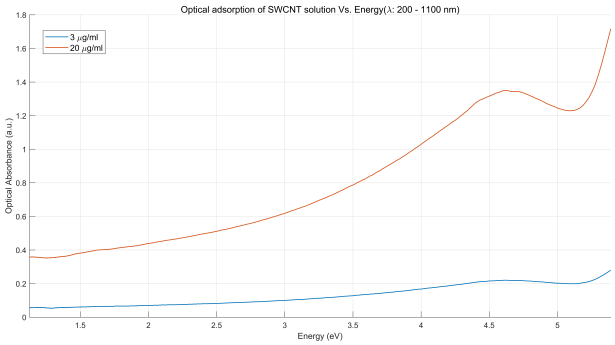

(a) Optical absorption spectra of SWCNT solutions in range of λ = 200 - 1100 nm

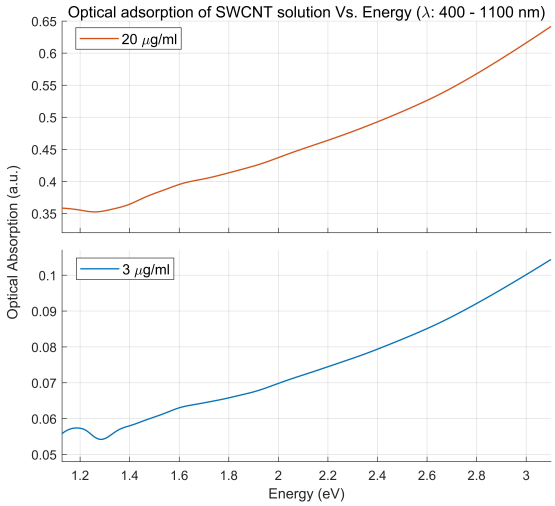

(b) Optical absorption spectra of SWCNT solutions in range of λ = 400 - 1100 nm

Figure 3.4: Optical absorption spectra of SWCNT solutions in different range of λ or photon energy

1. The first step was to dispense 150 ml of solutions onto the substrate. In this work, we used static dispensation process. Before spin coating process, the solutions covered all area on substrates as in figure 3.5.
2. The protocol of spin coating consisted of spin speed, spin acceleration, and spinning time. This protocol was applied in fabrications of SWCNT films with all of the concentrations in table 3.2.
   - **Step 1:** Spin speed = 300 rpm, Spin acceleration = 150 rpm/s,time = 15 s
   - **Step 2:** Spin speed = 1000 rpm, Spin acceleration = 500 rpm/s, time = 60 s
3. All samples were then heated at 70 - 80 degree Celsius for 15 minutes to remove some excess water in films.

3. Protocol for poly(vinyl alcohol) coating

- PVA solution was prepared from PVA powder (Mw: 89,000 - 98,000 g/mol) utilizing polymerization in water.
- 0.25 mM PVA solution was used to coat SWCNT thin films.
- Spin coating protocol

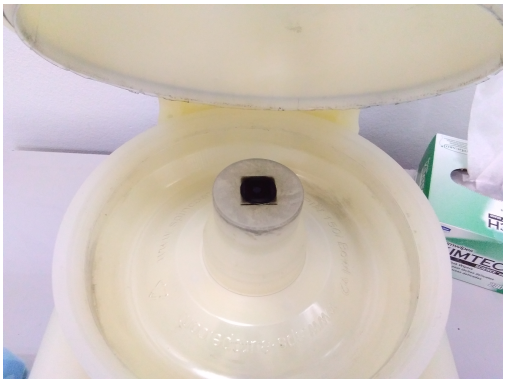

Figure 3.5: SWCNT solution dispensed on and covering over a glass substrate

- **Step 1:** Spin speed = 300 rpm, Spin acceleration = 150 rpm/s,time = 15 s
- **Step 2:** Spin speed = 1200 rpm, Spin acceleration = 600 rpm/s, time = 60 s

3.1.3 Preparation of Contacting Electrodes

To perform electrical measurement on the films, contacting electrodes are required. DC sputtering technique was used to fabricate electrodes.

Symmetrical electrode configuration

1. **Patterning method** is shown in figure 3.6. 1.3 cm × 2 cm glass slide was covered with copper foil and then put on the substrate to protect a certain area of SWCNT films.

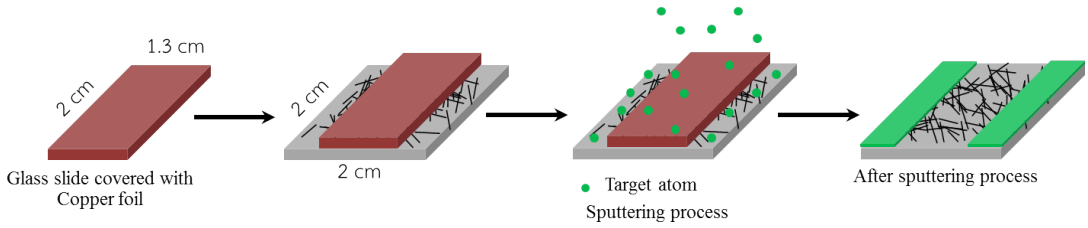

Figure 3.6: Diagram illustrating of patterning method for symmetrical electrode configuration

2. **Sputtering protocol**

   Before sputtering process, SWCNT films fabricated on glass substrates were kept at room temperature and atmospheric pressure at least 24 hours.The target materials used in this work were Ag and Cu. Specific values of parameter sets were required in sputtering process to deposit different target materials as shown in table 3.3.The distance between a target and substrate holder was always fixed.

Asymmetrical electrode configuration

The electrode patterning for the fabrication of asymmetrical electrode configuration is shown in figure 3.7. The sputtering protocol or parameter setting was the same as in table 3.3

Target	Sputtering pressure (Pa)	Pre-sputtering time (s)	Plasma current (mA)	Sputtering time (s)
Copper (Cu)	16 - 17	180	20	1200
Silver (Ag)	15	30 -60	20	1200

Table 3.3: Protocol of sputtering process with Copper and Silver target

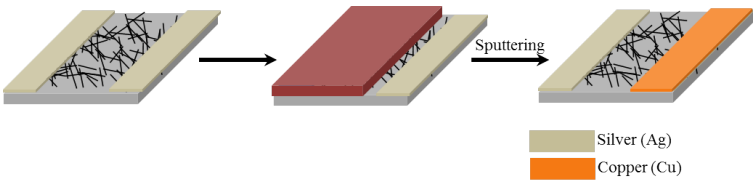

Figure 3.7: Diagram illustrating patterning method for symmetrical electrode configuration

3.1.4 Characterization of Carbon Nanotube Thin Films

Optical characterization (Film transmittance)

Film transmittances were calculated from the power of incident light and transmitted light through a sample at a specific wavelength. % Transmittances of films were calculated by the following equation.

$$Transmittance(\%) = \frac{\text{Power of transmitted light}}{\text{Power of incident light}} \times 100$$

The power of light was detected and measured with a silicon detector and Newport optical power meter, respectively. In this work, the measurements were performed at 750 nm - incident light. The 750 nm - incident light was generated from QTH (Quartz Tungsten Halogen) light source with a 750-nm bandpass filter. The instrument setup is shown in figure 3.8 except that the measurement is done in an aluminum box.

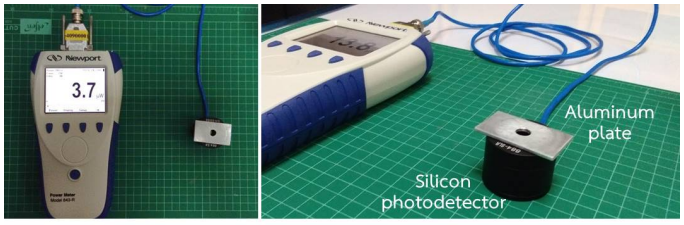

Figure 3.8: Experimental set up for transmittance measurement

Electrical characterization

1. *Current - Voltage (IV) characterization*

   IV measurement was done under ambient light with and without light illumination at room temperature and atmospheric pressure. The light illumination source was from QTH light source. As shown in figure 3.9 two-point probe method was employed to

measure current and voltage through SWCNT films. The power used to generate light source was 200 W. Note that it was not the power of light impacting samples. 2450-Keithley source meter was operated through kickstart program. Film resistances were used to characterize the properties of thin films. It is calculated by the following equation (ohm's law) at a specific voltage point or determining the slope of IV graph.

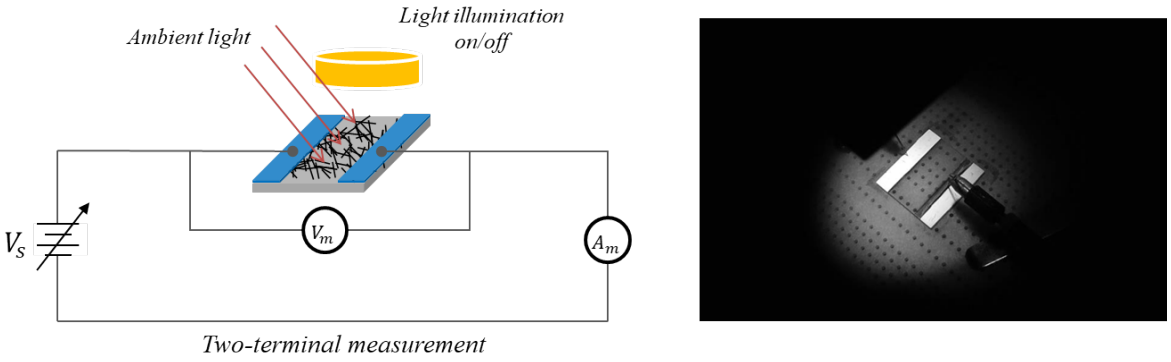

Figure 3.9: Current - voltage measurement circuit diagram

2. *Voltage - time response*

Voltage - time response was measured by using Agilent 3000 X-series oscilloscope which acted as both function generator and oscilloscope. A square wave signal was used in this work. The scheme of operation and circuit is shown in figure 3.10. Following the circuit diagram, the voltage signal was obtained at the sample or SWCNT thin film.

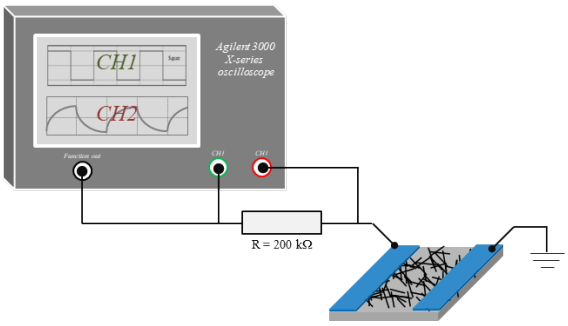

Figure 3.10: Voltage - time response measurement circuit diagram

The signal frequency was varied in the range of 10 Hz to 1 kHz. The amplitude of square wave signal was 1 V with $V_{p\text{-}p} = 2V$. So, the voltage was in the range of -1 V to 1 V. Time response, τ, could be determined from the voltage response graph by fitting curve with the following equation.

$$V = V_0 + Ae^{-t/\tau}$$

Where V_0 is amplitude of square wave signal, A is a constant, and τ is time response. From this equation, τ was defined as the time that the system takes in order to get to the assigned value of voltage.

3.2 Supercapacitors Based On Single - Walled Carbon Nanotube electrodes

3.2.1 Fabrication of superapacitor based on single - walled carbon nanotube electrode

To produce supercapacitor, we need to fabricate SWCNT thin films to act as electrodes in supercapacitor and gel electrolytes to separate SWCNT electrodes. The preparation and assembly of a supercapacitor is shown in figure 3.11.

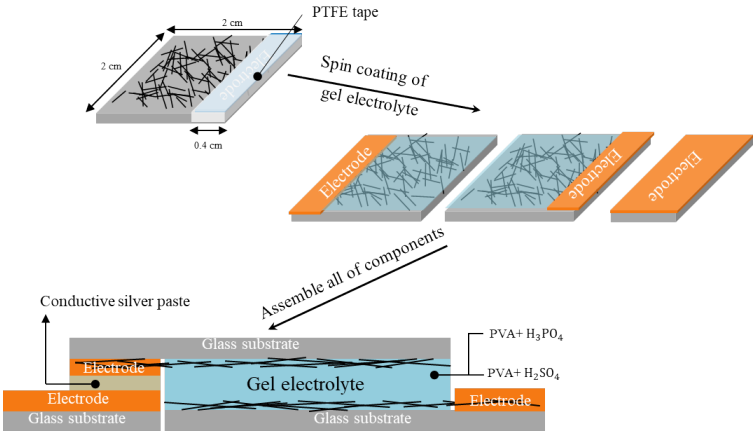

Figure 3.11: Diagram illustrating preparation of supercapacitor based on SWCNT electrode

Single - walled carbon nanotube electrodes were fabricated in the same way as single walled – carbon nanotube thin films with 0.6 mg/ml SWCNT concentration but there was only one contacting electrode as shown in figure 3.11. In this work, gel electrolytes were made of PVA solution and a certain type of acid. We used sulfuric acid and phosphoric acid to prepare different gel electrolytes. The mass proportion of PVA content and acid in gel electrolyte solution was 1:2. Before gel electrolyte was coated on SWCNT film, contacting electrodes had to be covered with PTFE tape to protect them from acid corrosion. Spin coating protocol for gel electrolytes coating was as following.

- **Step 1:** Spin speed = 300 rpm, Spin acceleration = 150 rpm/s,time = 15 s
- **Step 2:** Spin speed = 1500 rpm, Spin acceleration = 750 rpm/s, time = 60 s

3.2.2 Characterization of superapacitor based on single - walled carbon nanotube electrode

Cyclic voltammetry (CV)

Normally, cyclic voltammetry was done on three – electrode devices or electrochemical cells. The three electrodes are working electrode (WE), reference electrode (RE), and counter electrode (CE). The configuration of our supercapacitor cell is two – electrode device. However, we still can perform the measurement using the circuit shown in figure 3.12

to determine device capacitance. Keithley 2450 Source meter SMU was used to perform this measurement.

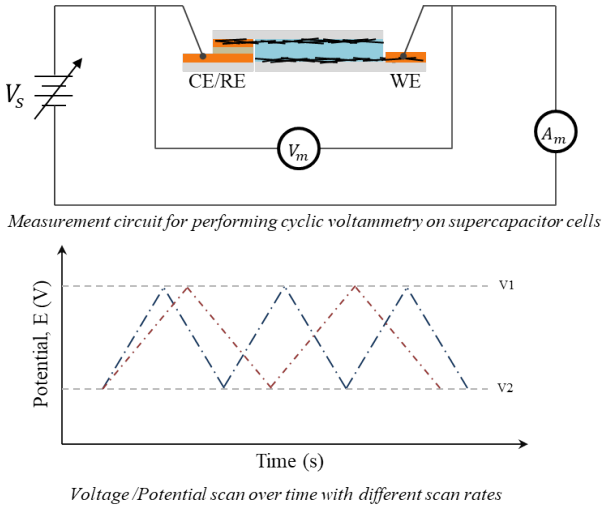

Figure 3.12: Cyclic voltammetry measurement circuit diagram and example of voltage scanning graph

Direct leakage current measurement

Leakage current can be modeled as a resistor that is parallel with a capacitor. This model is a simplification of the voltage and time dependence of leakage current. To perform direct leakage current measurement, we applied a fixed voltage to the device and then measured the resulting current for an amount of time. The leakage current measurement circuit diagram is shown in figure 3.13.

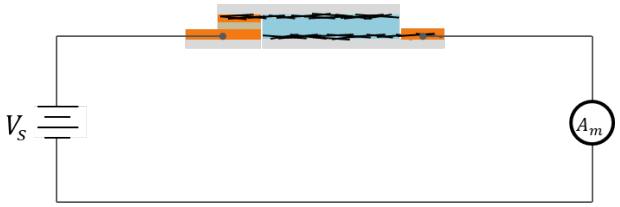

Figure 3.13: Measurement circuit of leakage current measurement on supercapacitor cells

Result and Discussion

4.1 Single - Walled Carbon Nanotube Thin Films

The studies on single - walled carbon nanotube thin film properties and characterizations were discussed in this section. They were divided into four main parts. In figure 4.1, some examples of SWCNT thin films are shown. It could be clearly seen that there was PVA layer covered SWCNT thin film in the bottom - left in figure 4.1. In addition, there was an overlay of different electrode material on SWCNT thin film with asymmetrical electrode configuration.

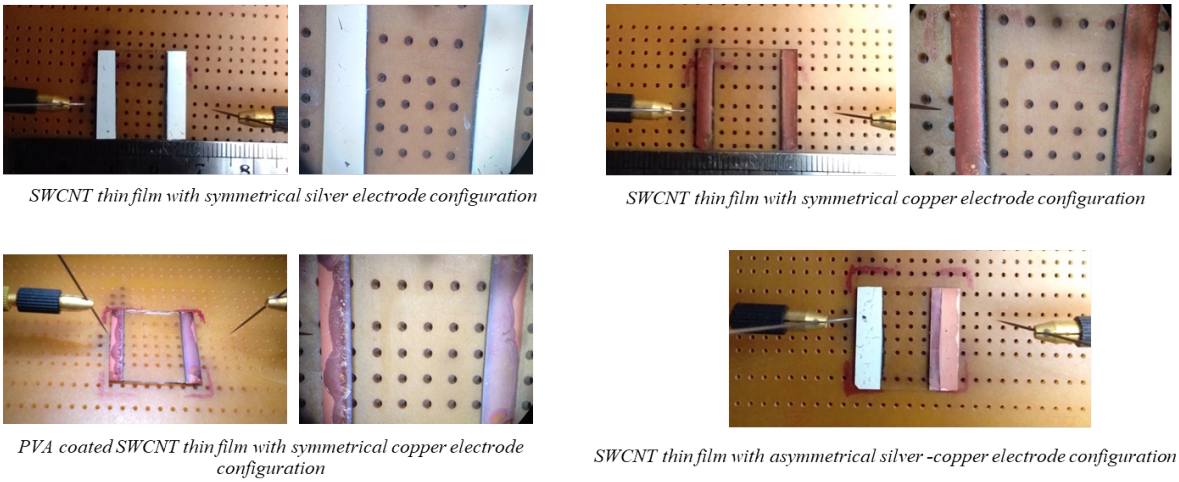

Figure 4.1: SWCNT thin film samples with different device configurations and structures

The notations with subscriptions "0" and "I" indicate value obtianedfrom the measurement under ambient light and light illumination, respectively.

4.1.1 Transmittance, Resistance, and Voltage response of SWCNT Thin Films

From table 4.1, transmittances of SWCNT thin films were increased as SWCNT concentration used in thin film fabrications were decreased. This indicated that the thickness and denseness of SWCNT thin film were changed as SWCNT concentration was varied. It was following the equation 2.3 as we expected. We also observed the change in film resistance with the variation of film thickness and denseness. As film transmittance was gradually increased, the resistance of SWCNT thin film was drastically increased. The rise in film resistance meant that the SWCNT thins film became less conductive. It is because fewer SWCNTs in the network could form conducting paths. We also noticed that resistance changes between S32 and S11 samples were very small compared to other samples in which the changes were in the order of magnitude. This might be because of the saturation of single - walled carbon nanotubes in film networks and the number of contact between SWCNTs and electrodes. Besides, there was a trend in voltage - time response of SWCNT thin films.

As film thickness and denseness were decreased which made films became more insulated, the responses of SWCNT thin films to a voltage tended to be slower.

SWCNT thin films fabricated in this work could be considered as transparent films because even with the highest concentration of SWCNTs, film transmittance were still as high as 80 percent including a glass substrate. From the result, we could manipulate the properties of SWCNT thin films by changing the solution concentration used in the fabrication process.

	Cu – Cu electrode					
	Batch1			*Batch 2*		
	%Transmittance	R_0 (MΩ)	τ (ms)	%Transmittance	R_0(MΩ)	τ (ms)
S32	88.873	0.072	0.036	87.828	0.069	0.027
S11	89.737	0.08	0.037	89.021	0.045	0.029
S12	90.931	0.237	0.06	91.599	0.304	0.067
S15	92.840	12	0.28	92.840	2.86	0.24
S110	93.079	116	-	93.000	17	-
Glass	94.988					

Table 4.1: Film transmittance, resistance, and voltage response of each sample in each batch

In figure 4.2, IV characteristics of various SWCNT thin films were shown. Most of the samples shown the linearity in IV curve at room temperature except for S110 sample in batch 1. It demonstrated the non-linearity in electrical behavior [figure 4.2a] while this behavior was not presented in S110 sample in batch 2 [figure 4.2b]. This might be because of the uncertainty and randomness in SWCNT network from the fabrication process or spin coating. So, we could not completely control the formation and pattern of SWCNTs in SWCNT thin films. However, this result can lead to an explanation about the electrical behaviors of SWCNT thin films. The linearity in IV characteristics was mostly shown in the thicker and denser film. Since there were both metallic and semiconducting SWCNTs in the networks, we suggest that there were more percolating or conducting paths formed by metallic tubes in thicker and denser films which made them more conductive. On the other hand, in the thinnest SWCNT thin film, there were less conductive paths formed and so the electrical behaviors of semiconducting SWCNTs dominated [18].

4.1.2 Electrical characteristics of SWCNT thin films with different electrode configurations

In this section, we had studied the effect of electrode configuration on electrical behaviors or IV characteristics of SWCNT thin films. For symmetrical electrode configuration with copper and silver shown in figure 4.2 and 4.3, IV characteristics of S11, S12, and S15 were linear which following ohm's law. Besides, SWCNT thin films with Ag - Cu asymmetrical electrode also showed the linearity in IV characteristic curves. This makes sense since there are no non - linearity behaviors presented in both SWCNT thin films with Cu and Ag electrodes. We also suggest that the role of the electrode in SWCNT networks is absent in our

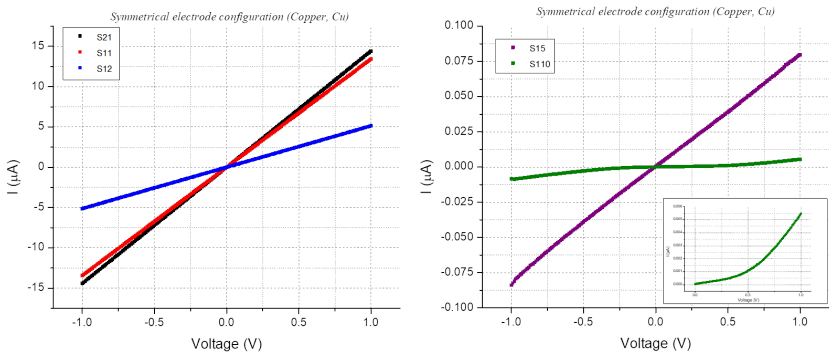

(a) IV characteristics of SWCNT thin films with Cu electrode in batch 1

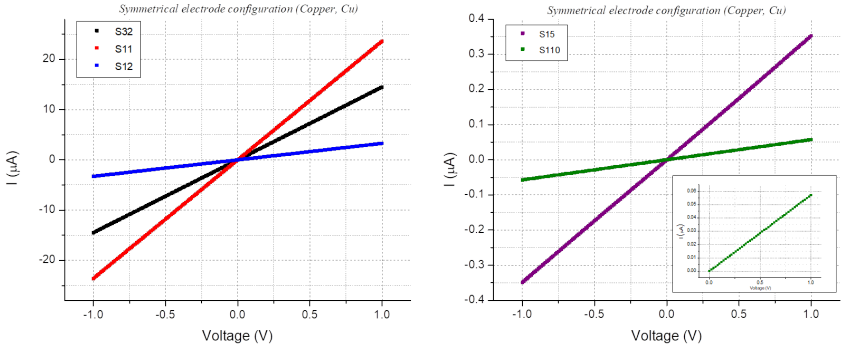

(b) IV characteristics of SWCNT thin films with Cu electrode in batch 2

Figure 4.2: IV characteristics of SWCNT thin films with Cu symmetrical electrode in each batch

cases and the electrical characteristics are mostly dominated by SWCNT films themselves.

4.1.3 Effects on electrical behavior of SWCNT thin films from Poly(Vinyl Alcohol) Polymer

Since we want to utilize these SWCNT thin films in optical sensing applications which is sometimes used in the real environment, a protective layer should be required to prevent SWCNTs in the networks from degradation. In this work, Poly(Vinyl Alcohol) polymer was used as a protective layer. So, we studied the effect of this protecting layer on SWCNT thin film's electrical behaviors.

After SWCNT thin films were coated with PVA, film resistances and time responses were increased in every sample as shown in table 4.2. Moreover, it could be seen from the decreasing of IV curve slopes in figure 4.5. This indicated that SWCNT thin films became more insulated corresponding to the properties of PVA which is an insulator. Being the networks composed of particles, SWCNT thin films is not bulk material. So, PVA molecules can penetrate between each nanotube and might block some conducting paths formed by these tubes. The rises in film resistances were approximately double of bare film resistances. However, PVA protective layer did not affect the linearities in IV characteristics of SWCNT thin films.

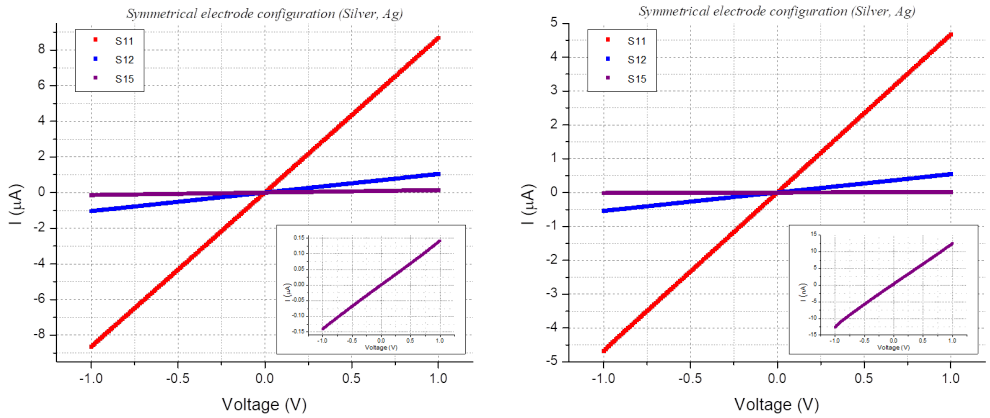

Figure 4.3: IV characteristics of SWCNT thin films with Ag symmetrical electrode in each batch

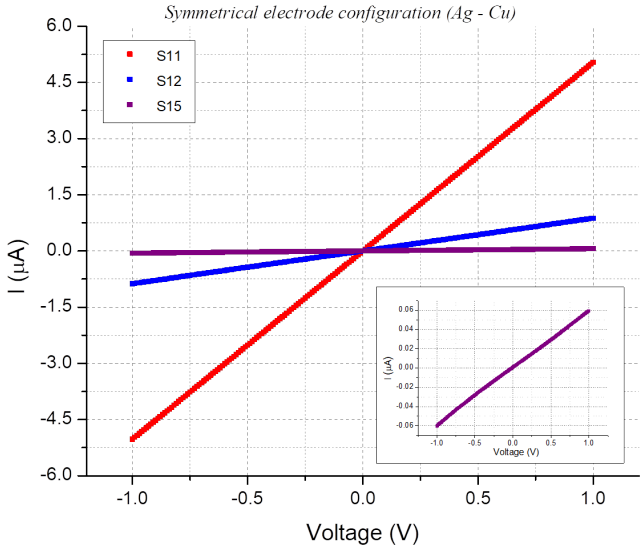

Figure 4.4: IV characteristics of SWCNT thin films with Ag - Cu asymmetrical electrode

4.1.4 Electrical characteristics of SWCNT thin films under light illumination

In this part, we discussed the response to the light illumination of bare and PVA coated SWCNT thin films. For the quick reminder, the light illumination used in this study was generated from QTH light source with power = 200 W and with a broad wavelength in the range of 200 nm to 2000 nm. Film resistances and IV characteristics of SWCNT thin films were studied under ambient light and light illumination.

In batch 1 and batch 2 samples, most bare SWCNT thin film resistances increased and slopes of IV curve decreased [figure 4.6] except for S15 sample which we would talk about it rather. For S32, S11, and S12 samples, if we illuminate them and then detect the resulting current, we should observe the decrease in the current. In contrast with S15 sample, the resulting current will increase after light illumination. The largest current difference detected

Cu – Cu electrode						
	Bare film		*PVA coated film*		ΔR (MΩ)	% Δ R/R_{bare}
	R_{bare} (MΩ)	τ_{bare} (ms)	R_{pva} (MΩ)	τ_{pva} (ms)		
S32	0.069	0.027	0.134	0.044	0.065	94
S11	0.045	0.029	0.104	0.037	0.059	131
S13	0.304	0.067	0.681	0.13	0.377	124
S15	2.83	0.24	5.52	0.28	2.69	95

Table 4.2: Comparison of electrical characteristics of SWCNT thin films before and after PVA coating

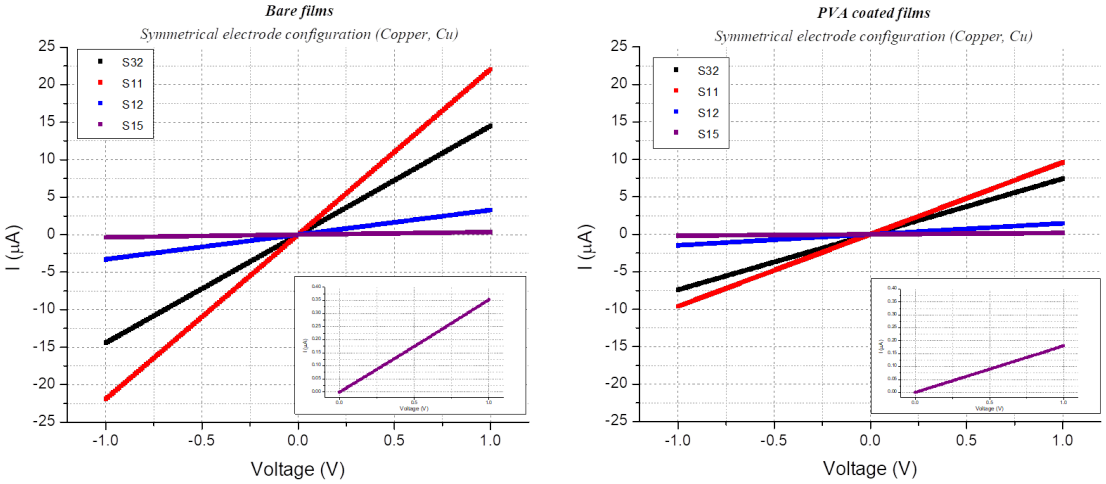

Figure 4.5: IV characeristics of SWCNT thin films before and after coated by PVA

at 1V - voltage was 6.5 μA obtained from S11 sample in batch 2 [figure 4.3]. Large current differences were derived from more conductive and thicker films. Considering the percent change in film resistance, there was no trend throughout the variation of SWCNT thin films.

Cu – Cu electrode, Bare films										
	Batch 1					*Batch 2*				
	R_0 (MΩ)	R_I (MΩ)	ΔR (MΩ)	ΔI at 1V (μA)	% ΔR/R	R_0 (MΩ)	R_I (MΩ)	ΔR (MΩ)	ΔI at 1V (μA)	% ΔR/R
S32	0.072	0.082	+0.01	-1.5	14	0.069	0.089	+0.02	-3.2	29
S11	0.08	0.11	+0.03	-2.9	37	0.045	0.064	+0.019	-6.5	42
S12	0.237	0.316	+0.08	-1	33	0.304	0.332	+0.03	-0.28	9
S15	12	8	-4	+0.04	33	2.86	2.62	-0.24	+0.03	8

Table 4.3: Comparison of electrical characteristics of bare SWCNT thin films under ambient light and light illumination

After SWCNT thin films were coated with PVA, we noticed that the response of PVA coated film to light was very different from the bare film. Under light illumination, film resistances, and IV curve slope [figure 4.7] of PVA coated film were all decreased and risen, respectively. This means that if we put PVA coated SWCNT films under light illumination, they will become more conductive, and the resulting current will be increased [table 4.4]. The difference in light response might be arising from the PVA layer or the change in SWCNT

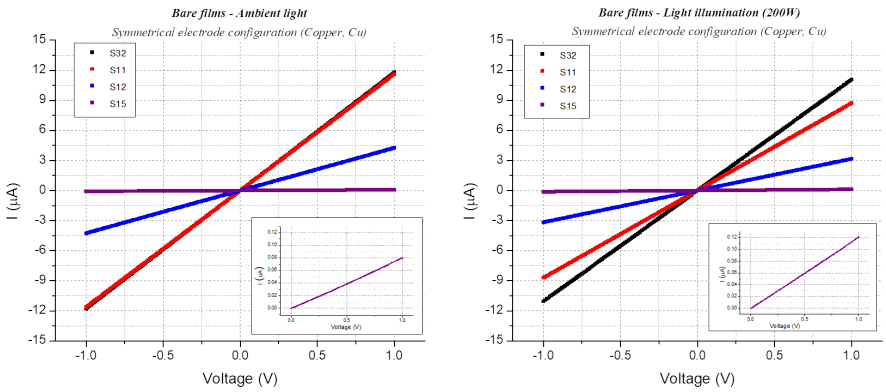

(a) Batch 1 (Left: under ambient light, Right: under light illumination)

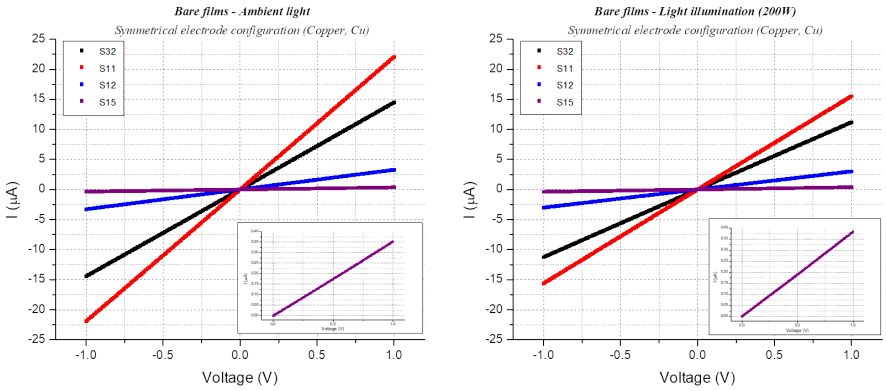

(b) Batch 2 (Left: under ambient light, Right: under light illumination)

Figure 4.6: IV characteristics of bare SWCNT thin films of each batch under ambient light and light illumination

properties caused by PVA which we do not know for sure. However, the current difference and percent change in resistance were not increased in S32 and S11 comparing to the result from bare films. Nevertheless, there were a significant rise in current difference and percent change in resistance detected from S12 and S15 sample. The highest percent resistance change of the sample from PVA coated film (S15) is higher than that of the sample from the bare film (S11).

Cu – Cu electrode, PVA coated films					
	R_0 (MΩ)	R_I (MΩ)	ΔR (MΩ)	ΔI at 1V (μA)	% ΔR/R
S32	0.0134	0.091	-0.043	+3.6	32
S11	0.104	0.098	-0.006	+0.5	6
S12	0.681	0.418	-0.263	+0.92	38
S15	5.5	2.9	-2.6	+0.158	47

Table 4.4: Comparison of electrical characteristics of PVA coated SWCNT thin films under ambient light and light illumination

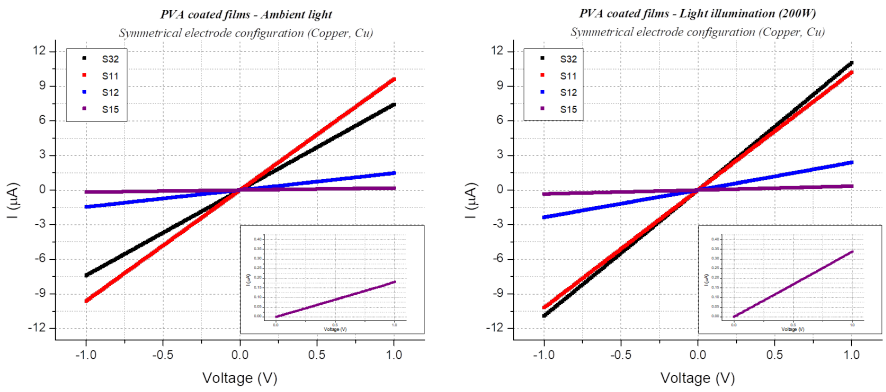

Figure 4.7: IV characteristics of PVA coated SWCNT thin films under ambient light (left) and light illumination (right)

4.2 Supercapacitors Based On single - walled carbon nanotube Electrode

4.2.1 Gel electrolyte: PVA - Sulfuric acid

In figure 4.8 (top left), CV curve showed the charge (ion absorption) and discharge (ion desorption) process. However, it was not symmetrical comparing both sides. This might be because some imperfections in the gel electrolyte or SWCNT electrode arising from the fabrication process. We have observed the difference in CV curve with different scan rates shown in figure 4.8 (top right and bottom left). Normalized current is defined as current normalized by scan rate. So, the area of normalized current CV curve is directly proportional to cell capacitance. The larger area under the normalized current CV curve, the higher capacitance.

From figure 4.8 (bottom right), it could be roughly concluded that capacitance with 70 mV/s scan rate was larger than with 140 mV/s scan rate. Following the equation 2.1 and 2.2, the capacitances obtained from 140 mV/s scan rate are 5.28 mF/m^2 and 1.58 μF. With 70 mV/s, the capacitances are 10.91 mF/m^2 and 3.275 μF. As we expected, capacitance from the lower scan rate was higher than the fast one. The leakage current of supercapacitor with PVA - H2SO4 gel electrolyte was about 10 nA.

Calculation of capacitance

- Scan rate (ν): 140 mV/s

  Area under CV curve = 4.434 $\times$ 10^{-7} μA·V, S = 3 cm^2, ΔV = 2 V

$$C_{s,140} = \frac{Area}{S\nu\Delta V}$$
$$= 5.28 \quad \text{mF/m}^2$$
$$C_{140} = SC_s = 1.58 \quad \mu\text{F}$$

- Scan rate (ν): 70 mV/s

  Area under CV curve = 4.585×10^{-7} μA·V, S = 3 cm^2, ΔV = 2 V

$$C_{s,70} = 10.91 \quad \text{mF/m}^2$$
$$C_{70} = SC_s = 3.275 \quad \mu\text{F}$$

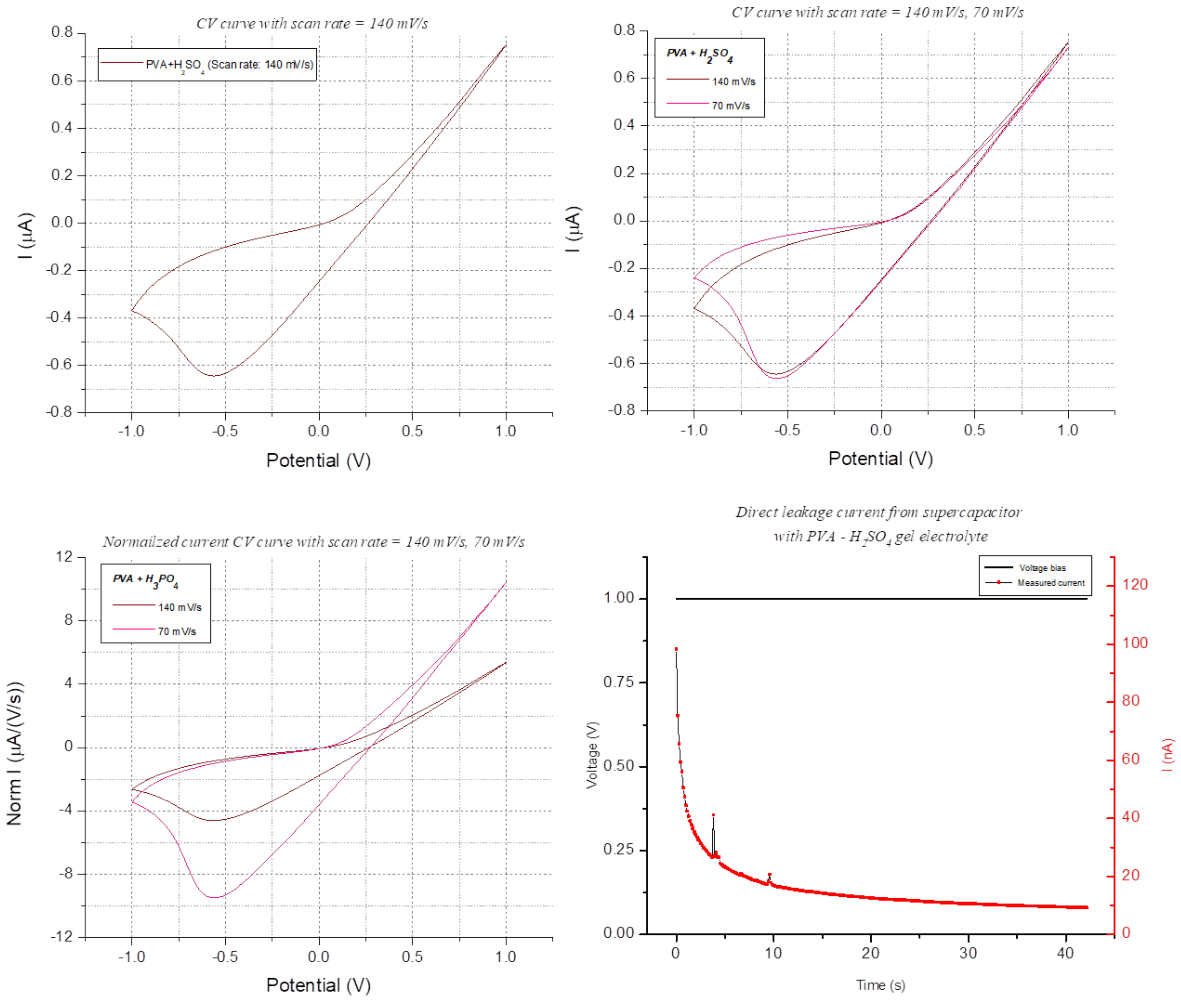

Figure 4.8: Characterizations of supercapacitor with PVA - H_2SO_4 gel electrolyte

4.2.2 Gel electrolyte: PVA -Phosphoric acid

CV curve of supercapacitor with PVA - H3PO4 showed charge and discharge process and was symmetrical with small shift in y - axis. The difference in CV curve with different scan rates was also observed. In normalized current CV curve [figure 4.9 - bottom left], capacitance with 105 mV/s scan rate should be higher than with 140 mV/s. The capacitances obtained from 140 mV/s scan rate are 24.5 mF/m^2 and 7.3 μF. With 105 mV/s, the capacitances are 30.6 mF/m^2 and 9.2 μF. The leakage current of supercapacitor with PVA - H2SO4 gel

electrolyte was about 1.25 μA.

Calculation of capacitance

- Scan rate (ν): 140 mV/s

  Area under CV curve = 2.06×10^{-6} μA·V, S = 3 cm^2, ΔV = 2 V

$$C_{s,140} = 24.5 \quad \text{mF/m}^2$$
$$C_{140} = SC_s = 7.3 \quad \mu F$$

- Scan rate (ν): 105 mV/s

  Area under CV curve = 1.93×10^{-6} μA·V, S = 3 cm^2, ΔV = 2 V

$$C_{s,105} = 30.6 \quad \text{mF/}m^2$$
$$C_{105} = SC_s = 9.2 \quad \mu\text{F}$$

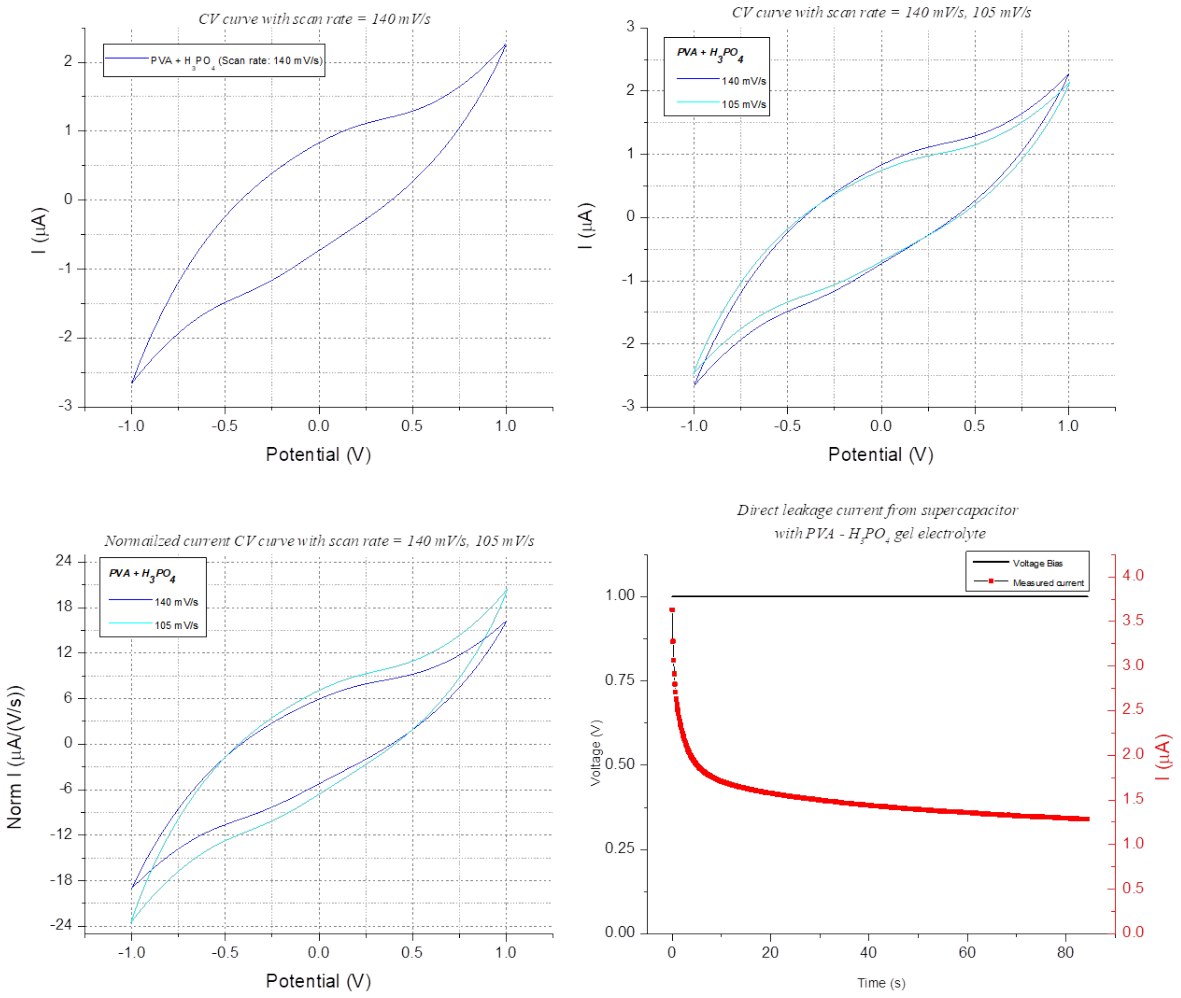

Figure 4.9: Characterizations of supercapacitor with PVA - H_3PO_4 gel electrolyte

4.2.3 Comparison of supercapacitors with different gel electrolytes

As we can see from figure 4.10, the area under CV curve of supercapacitor with PVA - H3PO4 gel electrolyte is larger and more symmetrical than with H2SO4. This might be because of more ions presented in PVA - H3PO4 gel electrolyte or the imperfection and defect in supercapacitor with PVA - H2SO4. However, the leakage current of supercapacitor with PVA - H3PO4 is higher than with PVA - H2SO4 in two orders of magnitude which means more power loss. This larger leakage current might lead to higher amounts of power loss because the stored charges are released from electrodes resulting in leakage current.

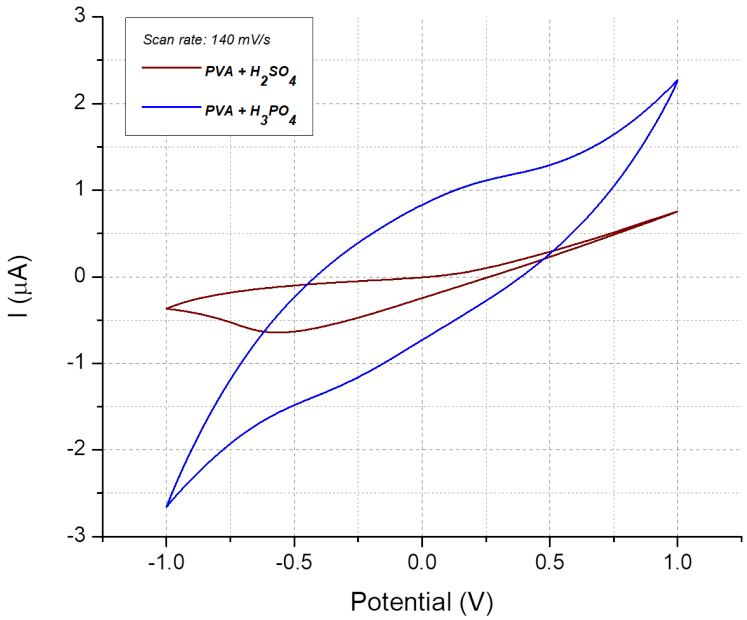

Figure 4.10: Comparison of CV curves from supercapacitors with different gel electrolyte

Conclusion

In this section, we conclude the whole of this study and its applications in this work. With very fascinating properties of single-walled carbon nanotubes in optical and electrical, we were drawn to study and investigate SWCNT based thin film for optical sensing and possibly for other applications. In this work, we mainly studied and characterized SWCNT thin films in aspects of electrical behavior and photodetection. Then, we demonstrated the use of SWCNT thin films as a high surface area electrode in electric double layer capacitor (EDLC), a type of supercapacitor. So, the study was divided into 2 parts, i.e., SWCNT thin films and supercapacitor based on SWCNT electrode.

The research on SWCNT thin films could be separated into 4 topics. The first one was the transmittance and electrical behavior of SWCNT thin films. We fabricated and characterized various SWCNT thin films from different SWCNT concentration. The result was as we expected the higher SWCNT concentration gave rise to the thicker, denser, and more conductive film indicated by lower optical transmittance. We observed that the linearity in IV characteristics representing the thicker film. As the film became thinner and thinner, the non - linearity was shown. So, from these results, we could manipulate and control the electrical properties of SWCNT thin films by varying the SWCNT concentration used in the fabrication or spin coating process.

We then studied the effect of electrode configuration on the electrical behavior of SWCNT thin film. In symmetrical electrode configuration, silver and copper were used. Silver and copper electrodes were then combined to get an asymmetrical electrode configuration. We found that there was no change in the linearity of IV characteristics with asymmetrical electrode configuration since there was only the linearity shown in both symmetrical electrode configuration, silver and copper. Next, the effect of poly(vinyl alcohol) polymer protective layer on SWCNT thin film property was observed. We found that SWCNT thin films became less conductive or more insulated which expressed from the increasing of film resistance. It is suggested that PVA might be able to penetrate and stuck in between tubes in SWCNT network resulting in less conductive paths formed by nanotubes following the fact that SWCNT thin films are not bulk materials.

The final study on SWCNT thin films was the electrical behavior changes of SWCNT thin film under light illumination. In both bare and PVA coated thin film, there was a change in resistance during light illumination but differently. For bare SWCNT thin films, the resistance of most samples increased under light illumination. The largest current difference was -6.5 μA at 1V - voltage with a 42 percent change in resistance. In contrast with the bare film, the resistance of PVA coated films decreased under light illumination which meant that they became more conductive. The highest percent change in resistance from PVA coated film was 47. However, the current differences were not significantly increased from the values obtained from thick bare films. With the change in resistance and current, SWCNT thin films might have the potential to be used as a photodetector. For example, if there is a change in the measured current over the film, then there is a change in light intensity. Moreover,

our SWCNT thin films can be considered as a broad wavelength photodetector.

Finally, we fabricated a more complex device, i.e., supercapacitor using SWCNT thin film based electrode. In this research, two types of gel electrolytes, i.e., PVA - H2SO4 and PVA - H3PO4, were studied. The capacitance of supercapacitor with PVA - H2SO4 electrolyte at 140 mV/s scan rate and 70 mV/s scan rate was 1.58 μF and 3.275 μF, respectively. The capacitance of supercapacitor with PVA - H3PO4 electrolyte at 140 mV/s scan rate and 105 mV/s scan rate was 7.3 μF and 9.2 μF. The charge - discharge mechanism was confirmed by the curve obtained from cyclic voltammetry.

Bibliography

[1] X. He, F. Léonard, and J. Kono, "Uncooled carbon nanotube photodetectors," *Advanced Optical Materials*, vol. 3, no. 8, pp. 989–1011, 2015. DOI: doi.org/10.1002/adom.201500237.

[2] S.Nanot, E. H. Hároz, J. Kim, R. H. Hauge, and J. Kono, "Optoelectronic properties of single-wall carbon nanotubes," *Advanced Materials*, vol. 24, no. 36, pp. 4977–4944, 2012. DOI: doi.org/10.1002/adma.201201751.

[3] L. Hu, D. S. Hecht, and G. Grüner, "Carbon nanotube thin films: Fabrication, properties, and applications," *Chemical Reviews*, vol. 110, no. 10, pp. 5790–5844, 2010. DOI: doi.org/10.1021/cr9002962.

[4] J. .-.-C. Charlier, X. Blaze, and S. Roche, "Electronic and transport properties of nanotubes," *Review of Modern Physics*, vol. 79, no. 2, pp. 677–711, 2007. DOI: doi.org/10.1103/RevModPhys.79.677.

[5] Ossila. (). Single-walled carbon nanotubes, [Online]. Available: https://www.ossila.com/products/single-walled-carbon-nanotubes?variant=34447448961.

[6] B. Adney. (2018). The structure and principle of electrical double layer capacitor, [Online]. Available: http://mylivelist.com/the-structure-and-principle-of-electrical-double-layer-capacitor.html.

[7] L. F. Aval, M. Ghoranneviss, and G. B. Pour, "High-performance supercapacitors based on the carbon nanotubes, graphene and graphite nanoparticleselectrodes," *Heylion*, vol. 4, no. 11, E00862, 2018. DOI: doi.org/10.1016/j.heliyon.2018.e00862.

[8] W. Chen, Z. Fan, L. Gu, X. Bao, and C. Wang, "Enhanced capacitance of manganese oxidevia confinement inside carbon nanotubes," *Chemical communication*, vol. 46, no. 22, pp. 3905–3907, 2010. DOI: doi.org/10.1039/C000517G.

[9] G. Z. Chen, "Understanding supercapacitors based on nano-hybrid materials with interfacial conjugation," *Progress in natural science: Material international*, vol. 23, no. 3, pp. 245–255, 2013. DOI: doi.org/10.1016/j.pnsc.2013.04.001.

[10] B. Pozo and et al., "Supercapacitor electro-mathematical and machine learning modelling for low power applications," *Electronics*, vol. 7, no. 4, p. 44, 2018. DOI: doi.org/10.3390/electronics7040044.

[11] M. Tyona, "A theorical study on spin coating technique," *Advances in Materials Research*, vol. 2, no. 4, pp. 195–208, 2013. DOI: doi.org/10.12989/amr.2013.2.4.195.

[12] Ossila. (). Spin coating: Complete guide to theory and techniques, [Online]. Available: https://www.ossila.com/pages/spin-coating.

[13] D. Meyerhofer, "Characteristics of resist films produced by spinning," *Journal of Applied Physics*, vol. 49, no. 7, pp. 3993–3997, 1978. DOI: doi.org/10.1063/1.325357.

[14] R. Hardeveld and et al., "Deposition of inorganic salts from solution on flat substrates by spin-coating: Theory, quantification and application to model catalysts," *Applied Surface Science*, vol. 84, no. 4, pp. 339–346, 1995. DOI: doi.org/10.1016/0169-4332(95)00010-0.

[15] A. G. Emslie, F. T. Bonner, and L. G. Peck, "Flow of a viscous liquid on a rotating disk," *Journal of Applied Physics*, vol. 29, no. 5, pp. 858–862, 1958. DOI: doi.org/10.1063/1.1723300.

[16] D. Depla, S. Mahieu, and J. E. Greene, "Sputter deposition process," in *A theoritical study on spin coating technique*, P. M. Martin, Ed., Elsevier Inc., 2010, ch. 5, pp. 253–296.

[17] M. Hughes. (2014). What is sputtering? magnetron sputtering? [Online]. Available: http://www.semicore.com/what-is-sputtering.

[18] V. Skákalová, A. B. Kaiser, Y.-S. Woo, and S. Roth, "Electronic transport in carbon nanotubes: From individual nanotubes to thin and thick networks," *PHYSICAL REVIEW B*, vol. 74, no. 8, pp. 085403-1 - 085403–10, 2006. DOI: doi.org/10.1103/PhysRevB.74.085403.